



Solvent suppression using phase-modulated binomial-like sequences and applications to diffusion measurements

Gang Zheng, Allan M. Torres, William S. Price *

Nanoscale Organisation and Dynamics Group, College of Health and Science, University of Western Sydney, Campbelltown Campus, Locked Bag 1797, Penrith South DC, NSW 1797, Australia

ARTICLE INFO

Article history:

Received 14 March 2008

Revised 16 May 2008

Available online 19 June 2008

Keywords:

Binomial-like sequences

Diffusion

Excitation sculpting

PGSE

Solvent suppression

WATERGATE

ABSTRACT

Two phase-modulated binomial-like π pulses have been developed by simultaneously optimizing pulse durations and phases. In combination with excitation sculpting, both of the new binomial-like sequences outperform the well-known 3-9-19 sequence in selectivity and inversion width. The new sequences provide similar selectivity and inversion width to the W5 sequence but with significantly shorter sequence durations. When used in PGSTE-WATERGATE, they afford highly selective solvent suppression in diffusion experiments.

© 2008 Elsevier Inc. All rights reserved.

1. Introduction

Since being introduced by Hore, binomial sequences [1,2], which have RF pulse durations in the ratio of binomial coefficients, have been widely used for selective excitation and inversion due to their good performance and ease of setup. To gain higher performance, binomial-like sequences (e.g., the 3-9-19 sequence [3] and W5 sequence [4]), which have the same symmetric pulse arrangement as binomial sequences but pulse durations in arbitrary ratios, have been developed by optimizing pulse durations using numerical methods. In combination with the WATERGATE sequence [5], binomial-like sequences provide an easy and efficient method of solvent suppression [3]. The phases of the RF pulses in binomial or binomial-like sequences are usually 0° or 180° [1–4]. However, for most modern NMR spectrometers, the phases of RF pulses can be controlled very accurately (e.g., to within 0.006°), which allows the employment of arbitrarily phased RF pulses (i.e., RF pulses with phases $= n \times (360^\circ/65536)$, $n = 0, 1, 2, 3, \dots, 65536$). Arbitrarily phased RF pulses have been employed in jump-return pulses for solvent and fat suppression [6,7]. No arbitrary phase combinations have previously been employed in binomial or binomial-like sequences due to the risk of introducing significant phase distortions. However, both excitation sculpting [8] and PGSTE-WATERGATE [9] sequences can remove phase distortions caused by the use of soft pulses. In this paper, two 6-pulse PM (Phase Modulated) binomial-like sequences with arbitrary phase combinations, which outperform the widely used 3-9-19 (also referred to as W3) sequence [3,4], have been ob-

tained, and the new binomial-like sequences have been combined with the excitation sculpting and PGSTE-WATERGATE sequences.

A brief introduction of the salient features of binomial and binomial-like sequences and planar rotations, which are required to develop and evaluate the sequences presented here, is given in the following section. The performance of the newly developed sequences is illustrated in combination with the excitation sculpting and PGSTE-WATERGATE methods on a sample containing 2 mM lysozyme in water ($10:90 \text{ D}_2\text{O}/\text{H}_2\text{O}$).

2. Theory

2.1. Binomial and binomial-like sequences

A general binomial-like sequence can be written as [2]

$$\alpha_1(\varphi_1) - \tau - \alpha_2(\varphi_2) - \tau \cdots \alpha_n(\varphi_n) - \tau - \alpha_n(\varphi_{n+1}) \cdots \tau - \alpha_2(\varphi_{2n-1}) - \tau - \alpha_1(\varphi_{2n}), \quad (1)$$

where α_i ($i = 1, 2, \dots, n$) is the nutation angle of the RF pulse, φ_i ($i = 1, 2, \dots, 2n$) is the pulse phase, and τ is the inter-pulse delay. Traditionally, the pulse phase is set as 0° or 180° , for example, the 1-3-3-1 [1,2] and 3-9-19 [3] sequences can be written as

$$45^\circ(0^\circ) - \tau - 135^\circ(0^\circ) - \tau - 135^\circ(180^\circ) - \tau - 45^\circ(180^\circ), \quad (2)$$

and

$$20.77^\circ(0^\circ) - \tau - 62.31^\circ(0^\circ) - \tau - 131.54^\circ(0^\circ) - \tau - 131.54^\circ(180^\circ) - \tau - 62.31^\circ(180^\circ) - \tau - 20.77^\circ(180^\circ), \quad (3)$$

respectively.

* Corresponding author. Fax: +61 2 4620 3025.

E-mail address: w.price@uws.edu.au (W.S. Price).

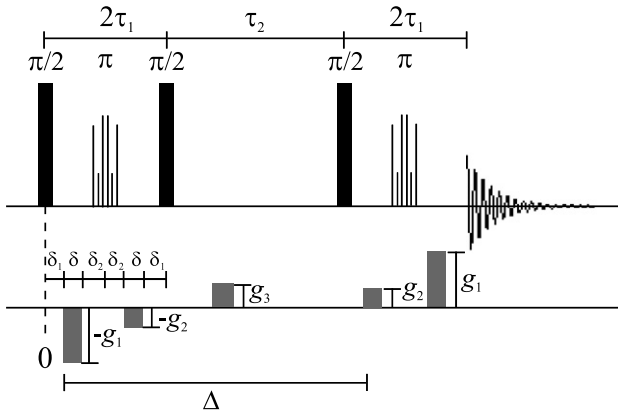


Fig. 1. The PGSTE-WATERGATE sequence with new binomial-like π pulses. The black columns represent $\pi/2$ RF pulses, and the groupings of narrow bars represent binomial-like π pulses, and g_1, g_2 and g_3 are rectangular gradient pulses with different amplitudes. The phase cycles for the first, second, third $\pi/2$ pulse, the first and second binomial-like sequences, and receiver are $\theta_1 = x, -x; \theta_2 = x, y, -x, -y; \theta_3 = x, y, -x, -y; \theta_4 = (x)_6, (x)_6, (y)_6, (y)_6, (-x)_6, (-x)_6, (-y)_6, (-y)_6; \theta_5 = (x)_6, \theta_r = y, -y, -y, y$. The phases of the pulses of the binomial-like sequences are given by $240.969^\circ - 320.652^\circ - 302.794^\circ - 122.794^\circ - 140.652^\circ - 60.969^\circ + \theta_4$ (or θ_5) (for PM1), and $214.524^\circ - 304.508^\circ - 304.530^\circ - 124.530^\circ - 124.508^\circ - 34.524^\circ + \theta_4$ (or θ_5) (for PM2).

In obtaining new binomial-like sequences, it is necessary to express the magnetization after the application of binomial-like sequences as functions of each pulse sequence elements. In this study, product operators [10] have been used to model the effects of the sequences.

2.2. Simulation of plane rotation

For most of the selective π RF pulses, the magnetization immediately before the pulse is on the transverse (i.e., $x - y$) plane. Especially in the WATERGATE [5] and WATERGATE-like sequences (e.g., excitation sculpting [8], PGSE-WATERGATE [11], and PGSTE-WATERGATE [9]), the magnetization right before the selective pulse has totally fanned out in the transverse plane, signifying that a selective π pulse has to invert the whole magnetization plane instead of just a magnetization vector. These selective π pulses can be called plane rotation pulses [12]. The simplest way to simulate a plane rotation is to use a vector perpendicular to the plane to track the movement of the magnetization plane. A magnetization vector initially on the positive z axis can simply do the job. An ideal π pulse rotates the magnetization vector from the positive z direction to the negative z direction.

In all simulations, the performance of the binomial-like π pulses has been assessed by calculating the final z magnetization caused

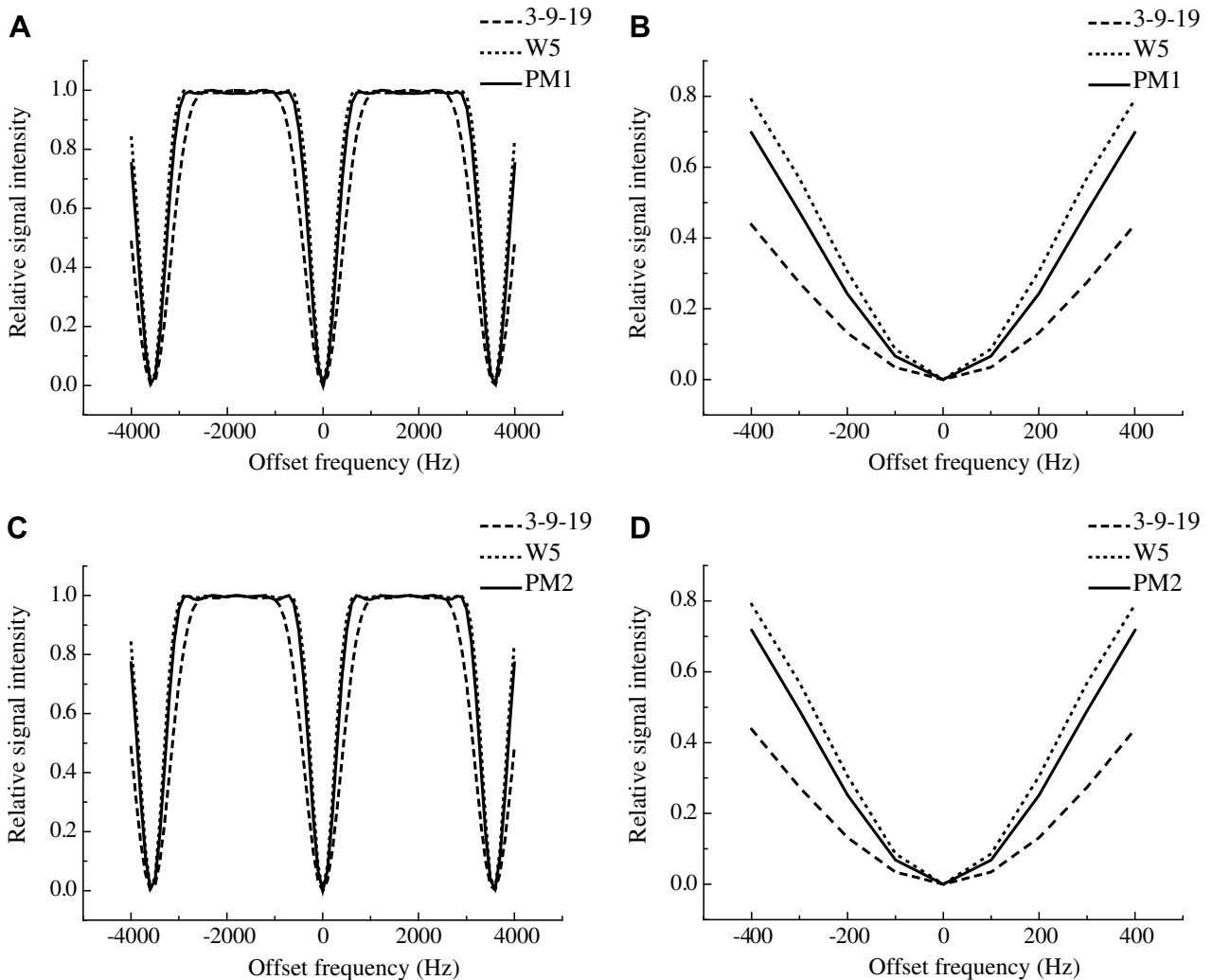


Fig. 2. Simulated inversion profiles of the PM1, PM2, W5 and 3-9-19 sequences with an inter-pulse delay of 280 μ s. It has been assumed that the power of RF pulses is high enough to make the resonance offset effects negligible during the application of RF pulses.

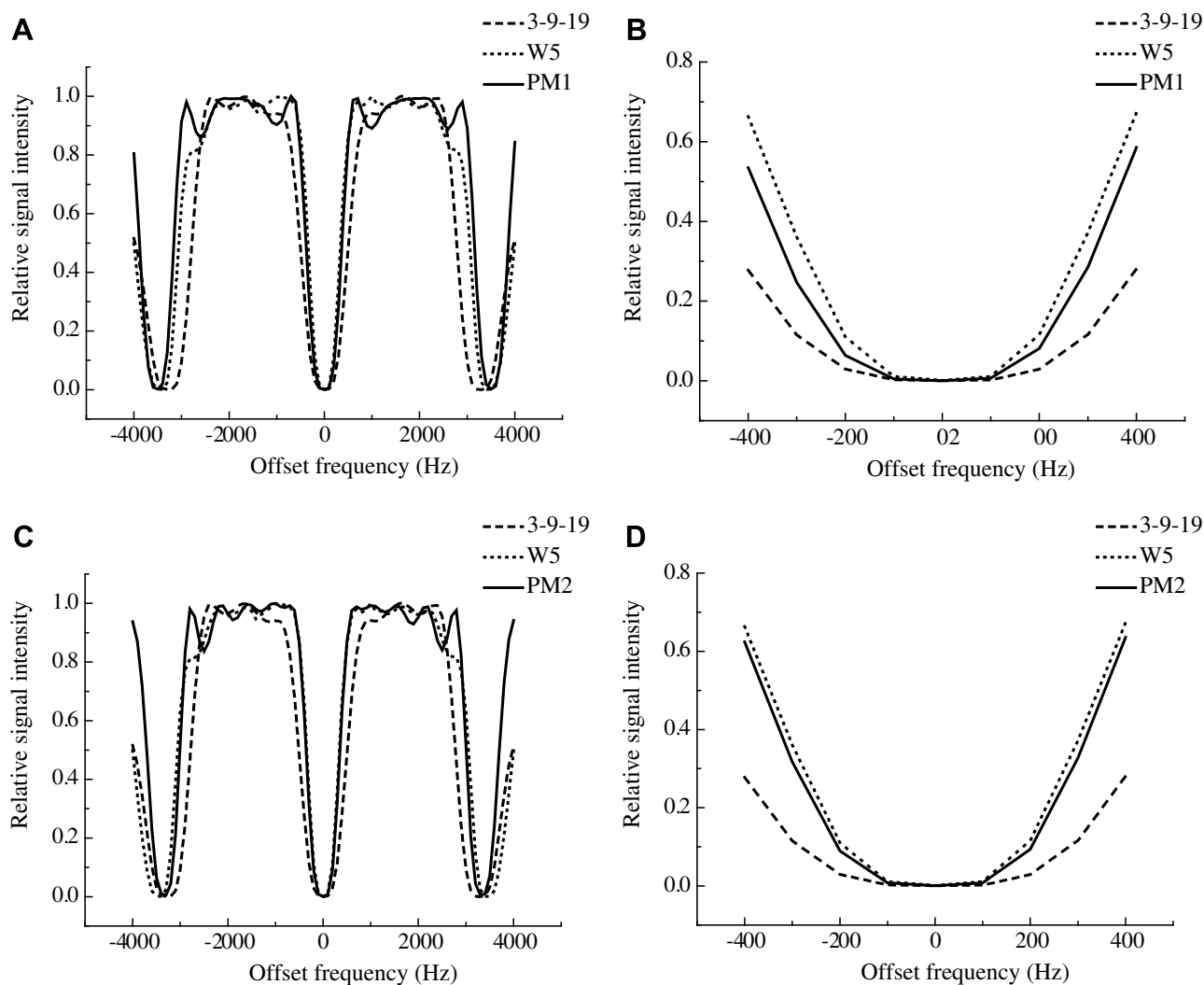


Fig. 3. Excitation sculpting excitation profiles of the PM1, PM2, W5 and 3-9-19 sequences using CuSO_4 -doped D_2O with $\gamma B_1/2\pi = 12$ kHz for binomial-like sequences and an inter-pulse delay of $280 \mu\text{s}$.

by applying the selective pulses to an initial positive z magnetization. Because z magnetization does not provide any phase information, the simulation mentioned above may generate selective pulses not only providing the desired inversion profile but also causing significant phase errors. Therefore, the new selective pulses must be used in conjunction with the excitation sculpting and PGSTE-WATERGATE sequences to remove the phase errors.

In general, there are two approaches for the development of binomial-like sequences: analytical methods (e.g., Fourier transform approximation [2] and rotation operator treatment [2]) and numerical methods [4,13,14]. Since this study is focused on the development of binomial-like sequences with the optimal inversion profiles, a numerical optimization procedure based on least-squares analysis has been employed.

2.3. PGSTE-WATERGATE

The diffusion-based attenuation of the non-solvent resonances in the PGSTE-WATERGATE sequence (Fig. 1) can be written as [9]

$$E = \exp \left\{ -\gamma^2 D \delta^2 \left[\left(\Delta - \frac{4}{3} \delta - 2\delta_2 \right) (g_1 - g_2)^2 + \frac{2}{3} \delta (g_1 - g_2) g_1 + \left(4\delta_2 + \frac{4}{3} \delta \right) g_1^2 \right] \right\}, \quad (4)$$

where D ($\text{m}^2 \text{s}^{-1}$) is the diffusion coefficient, and γ ($\text{rad s}^{-1} \text{T}^{-1}$) is the gyromagnetic ratio of the nucleus being used, and Δ , δ , δ_2 , g_1 and g_2 are defined in Fig. 1. In this study, the g_1 gradient in the PGSTE-WATERGATE sequence has been set larger than the g_2 gradient to make the “ $(g_1 - g_2) \times g_1$ ” term in Eq. (4) positive and the “ g_1^2 ” term greater, thereby enhancing the encoding efficiency of the applied gradients.

3. Experimental

Two samples were used to evaluate the new sequences: 2 mM lysozyme in water (10:90 $\text{D}_2\text{O}/\text{H}_2\text{O}$) was provided in a sealed NMR tube by Bruker (Karlsruhe, Germany) as the standard water-suppression sample, and CuSO_4 -doped D_2O (99.9 atom %D, ISOTEC, Matheson) was placed into a magnetic susceptibility-matched (to D_2O) NMR tube (BMS-003, Shigemi).

All experiments were conducted on a Bruker 500 MHz Avance NMR spectrometer at 25°C . The excitation sculpting profiles of the binomial-like sequences were obtained with gradient strengths of 0.185 T m^{-1} and 0.120 T m^{-1} for the first and second bipolar gradient pairs in the excitation sculpting sequence, respectively, and an inter-pulse delay, τ , of $280 \mu\text{s}$ for the binomial-like sequences. The excitation sculpting spectra of lysozyme were obtained using the excitation sculpting sequence with number-of-scans = 64,

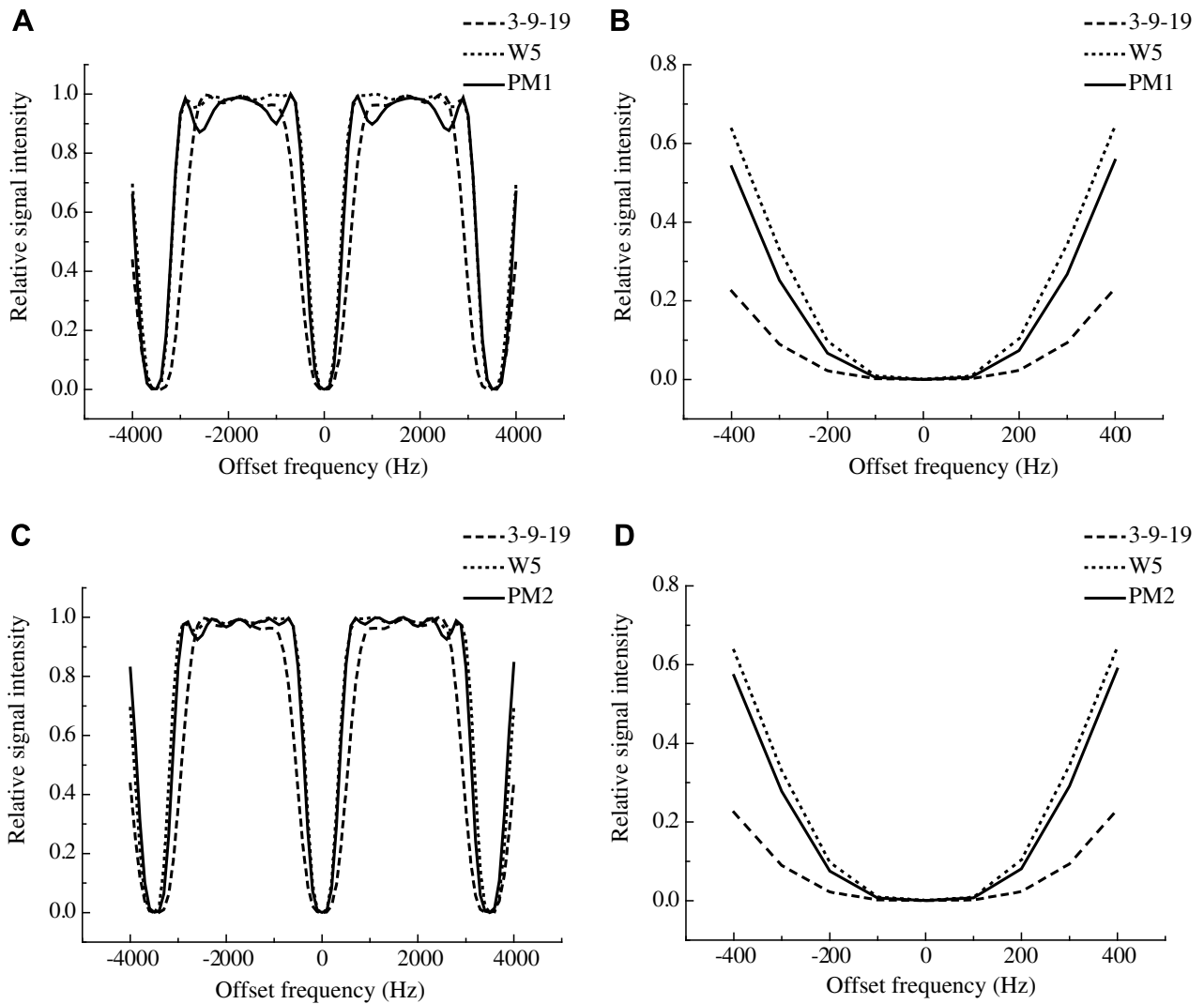


Fig. 4. Excitation sculpting excitation profiles of the PM1, PM2, W5 and 3-9-19 sequences using CuSO_4 -doped D_2O with $\gamma B_1/2\pi = 32$ kHz for binomial-like sequences and an inter-pulse delay of 280 μs .

two gradient strengths of 0.203 T m^{-1} and 0.072 T m^{-1} in combination with different binomial-like sequences with inter-pulse delay of 282 μs . The WATERGATE spectrum of lysozyme was

obtained using the WATERGATE sequence with number-of-scans = 64, a gradient strength of 0.195 T m^{-1} in combination with the PM1 sequence with inter-pulse delay of 282 μs .

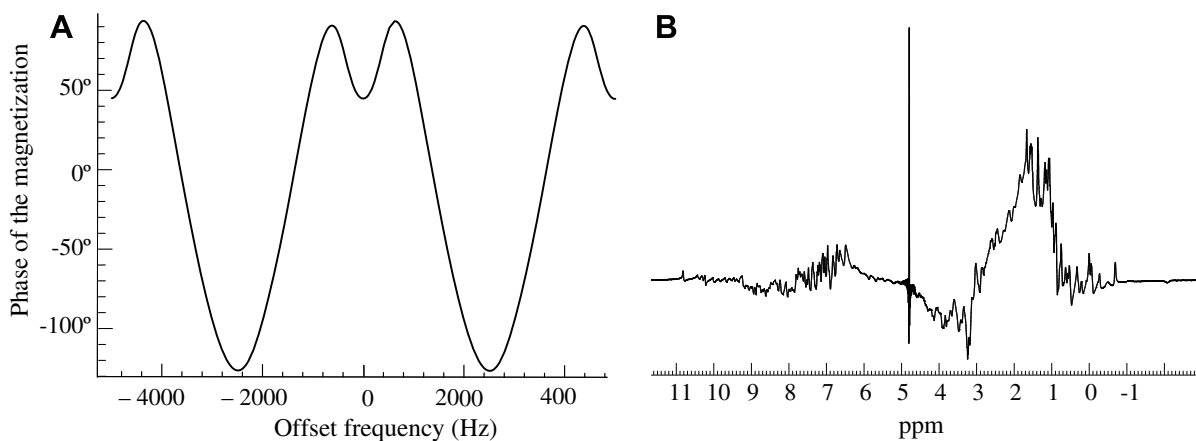
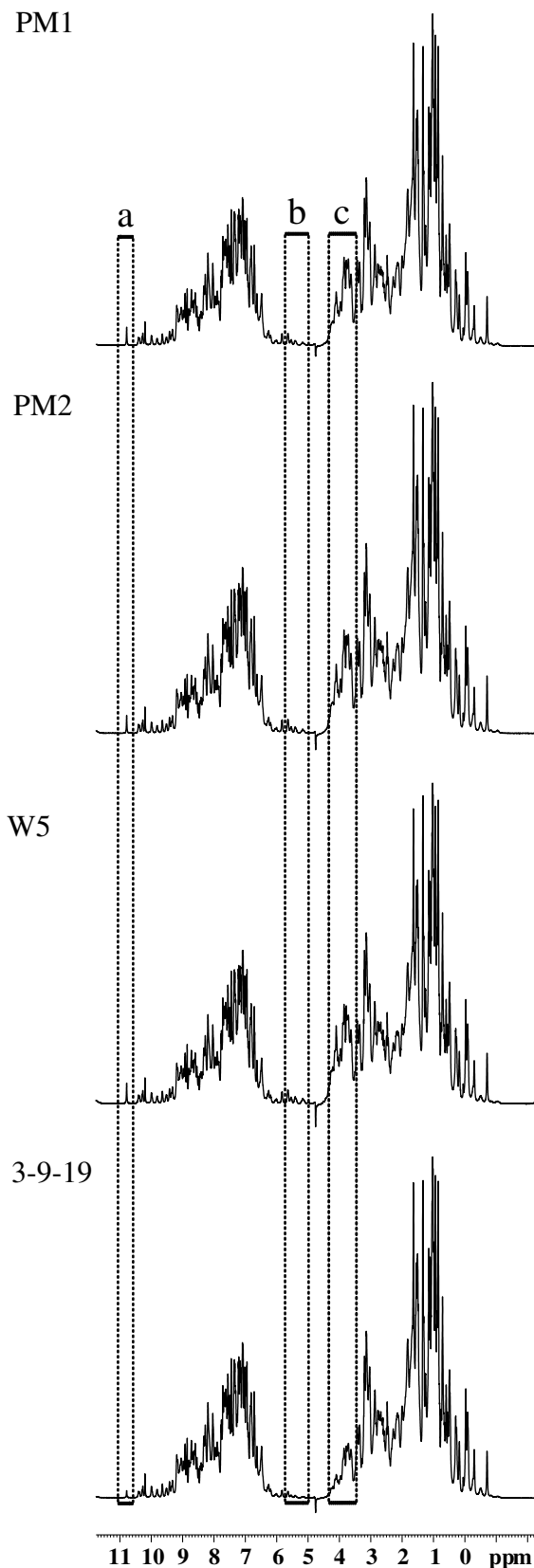


Fig. 5. (A) The phase of the final magnetization vector at different offset frequencies. (B) The ^1H WATERGATE spectrum of a sample containing 2 mM lysozyme in water (10:90 $\text{D}_2\text{O}/\text{H}_2\text{O}$) using a gradient strength of 0.195 T m^{-1} and the PM1 binomial-like sequence with an inter-pulse delay of 282 μs .

PGSTE-WATERGATE experiments were performed on lysozyme with number-of-scans = 32, g_1 varying from 0.159 T m^{-1} to 0.541 T m^{-1} , $g_2 = 0.131 \text{ T m}^{-1}$, $\delta = 4 \text{ ms}$, $\Delta = 62.2 \text{ ms}$, $\delta_1 = 0.05 \text{ ms}$, and $\delta_2 = 0.2 \text{ ms}$. All simulations were performed in Maple 11

(Maplesoft, Waterloo), and the Maple routine least-squares tool (LSSolve) was used for optimization. In all simulations, it was assumed that the power of the RF pulses was high enough to make the resonance offset effects during the application of the RF pulses negligible.



4. Results and discussion

The general form of a 6-pulse phase-modulated binomial-like sequence in this study can be written as [13]

$$\alpha(\varphi_1) - \tau - \beta(\varphi_2) - \tau - \gamma(\varphi_3) - \tau - \gamma(\varphi_3 + 180^\circ) - \tau - \beta(\varphi_2 + 180^\circ) - \tau - \alpha(\varphi_1 + 180^\circ). \quad (5)$$

To ensure that the on-resonance magnetization automatically goes back to the positive z axis (i.e., experiences a zero inversion), a 180° shift was added to the phase-pattern of the second half of the sequence [13]. For the on-resonance magnetization, the rotations caused by $\alpha(\varphi_1)$, $\beta(\varphi_2)$, and $\gamma(\varphi_3)$ are cancelled by the rotations caused by $\alpha(\varphi_1 + 180^\circ)$, $\beta(\varphi_2 + 180^\circ)$, and $\gamma(\varphi_3 + 180^\circ)$, respectively.

The desired selective inversion pulse has no effect on the on-resonance magnetization but inverts all off-resonance magnetizations inside the effective inversion width (i.e., z -magnetization (M_z) = $1 \rightarrow M_z = -1$). Therefore, in the simulations based on product operators, the sequence shown in sequence (5) has been applied to a magnetization along the positive z axis. The inter-pulse delay (τ) of the sequence has been set to $200 \mu\text{s}$ to give a bandwidth of 5000 Hz between the null points, and thus the z -component of the final magnetization has been calculated at five offset frequencies: 50 Hz , 1500 Hz , 2000 Hz , 3000 Hz , and 3500 Hz . Each of the three pulse durations (i.e., α , β , γ) has been manually set from 0° to 360° in increments of 30° before each optimization due to the limitation on the number of variables in the least-squares optimization tool of Maple 11. For example, for $\alpha = 60^\circ$, the final z -magnetization is a function of β , γ , φ_1 , φ_2 , φ_3 , and the offset frequency (Ω) (i.e., $f(\beta, \gamma, \varphi_1, \varphi_2, \varphi_3, \Omega)$). The sum-of-squares is given by

$$\begin{aligned} & (f(\beta, \gamma, \varphi_1, \varphi_2, \varphi_3, 50\text{Hz}) - 0)^2 + (f(\beta, \gamma, \varphi_1, \varphi_2, \varphi_3, 1500\text{Hz}) \\ & - (-1))^2 + (f(\beta, \gamma, \varphi_1, \varphi_2, \varphi_3, 2000\text{Hz}) - (-1))^2 \\ & + (f(\beta, \gamma, \varphi_1, \varphi_2, \varphi_3, 3000\text{Hz}) - (-1))^2 \\ & + (f(\beta, \gamma, \varphi_1, \varphi_2, \varphi_3, 3500\text{Hz}) - (-1))^2. \end{aligned} \quad (6)$$

The optimal combination of β , γ , φ_1 , φ_2 , and φ_3 has been found by minimizing the sum-of-squares shown above. The optimal combination of pulse durations and phases has been obtained for each of these manually set values. The sequences presented here have been selected from these combinations based on their inversion width and selectivity.

The newly obtained binomial-like sequences, PM1 and PM2, can be written as

Fig. 6. A series of $500 \text{ MHz } ^1\text{H}$ excitation sculpting spectra of a sample containing 2 mM lysozyme in water ($10:90 \text{ D}_2\text{O}/\text{H}_2\text{O}$) at 25°C using the PM1, PM2, W5 and 3-9-19 sequences. The inter-pulse delay, τ , in the binomial-like sequences was set to $282 \mu\text{s}$. The signal intensity in region a (signals due to NH protons), which is at the edge of each spectrum, reflects the inversion width of each binomial-like sequence. The significant signal attenuation in this region of the 3-9-19 spectrum indicates that the 3-9-19 sequence provides a smaller inversion width than the PM1, PM2 and W5 sequences, which provide similar inversion widths. The signal intensity in regions b and c (signals due to backbone H_α protons), which are right next to the water resonance, reflects the selectivity of each binomial-like sequence. In the PM1, PM2 and W5 spectra, the signal intensity in these regions is much higher than those in the 3-9-19 spectrum, indicating that the PM1, PM2, and W5 sequences are similar but more selective than the 3-9-19 sequence.

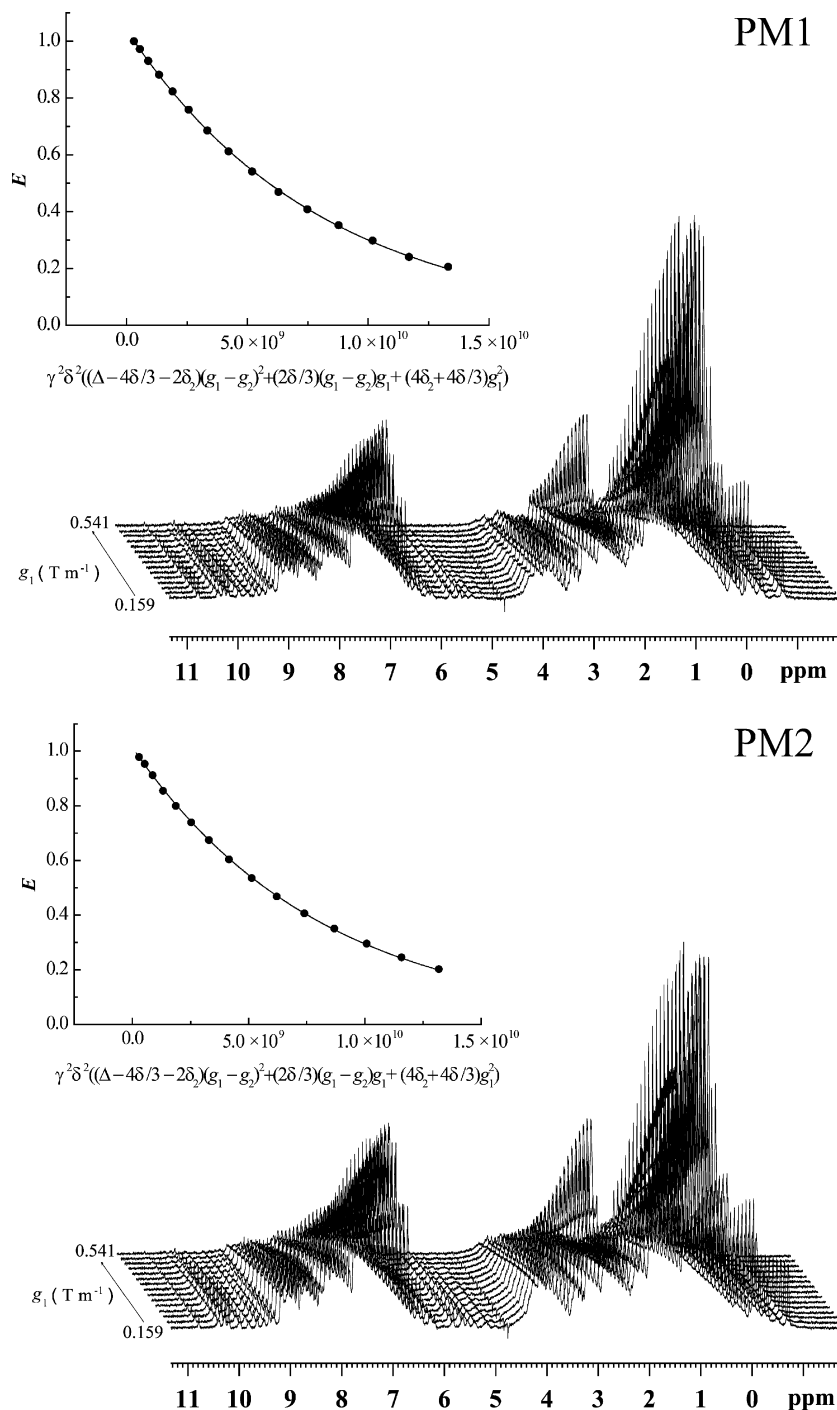


Fig. 7. A series of 500 MHz ^1H PGSTE-WATERGATE spectra of a sample containing 2 mM lysozyme in water (10:90 $\text{D}_2\text{O}/\text{H}_2\text{O}$) at 25 °C. The diffusion decays calculated from the spectra presented are also shown. The measured diffusion coefficients of lysozyme were, within experimental error, identical (i.e., $1.13 \pm 0.01 \times 10^{-10} \text{ m}^2 \text{ s}^{-1}$ (PM1) and $1.15 \pm 0.01 \times 10^{-10} \text{ m}^2 \text{ s}^{-1}$ (PM2)) by averaging the data obtained in three independent experiments for each sequence.

$$\begin{aligned}
 &260.47^\circ(240.969^\circ) - \tau - 120.00^\circ(320.652^\circ) - \tau \\
 &\quad - 313.04^\circ(302.794^\circ) - \tau - 313.04^\circ(122.794^\circ) - \tau \\
 &\quad - 120.00^\circ(140.652^\circ) - \tau - 260.47^\circ(60.969^\circ), \quad (7)
 \end{aligned}$$

and

$$\begin{aligned}
 &89.99^\circ(214.524^\circ) - \tau - 42.12^\circ(304.508^\circ) - \tau \\
 &\quad - 120.00^\circ(304.530^\circ) - \tau - 120.00^\circ(124.530^\circ) - \tau \\
 &\quad - 42.12^\circ(124.508^\circ) - \tau - 89.99^\circ(34.524^\circ), \quad (8)
 \end{aligned}$$

respectively. The simulated inversion profiles are shown in Fig. 2, and experimental excitation profiles for binomial-like sequences at different RF power levels are shown in Figs. 3 and 4. An interpulse delay of 280 μs was used for the simulations and experiments and this corresponds to a bandwidth of 3571 Hz between the null points. For the simulated profiles (Fig. 2), the resulting frequency widths which provide better than 90% inversion are 2500, 2525, 2640, and 2040 Hz for the PM1, PM2, W5, and 3–9–19 sequences, respectively, corresponding to an increase in the inversion bandwidth of 460 Hz for PM1 and 485 Hz for PM2, compared with the

3-9-19 sequence. The frequency width of the suppression region which produces less than 10% of the intensity are 240, 236, 214, and 336 Hz for the PM1, PM2, W5, and 3-9-19 sequences, respectively, which are equivalent to narrowing the suppression region by 28% for PM1 and 30% for PM2, compared with the 3-9-19 sequence. For the experimental profiles with $\gamma B_1/2\pi = 12$ kHz for binomial-like sequences (Fig. 3), the resulting frequency widths which provide better than 90% inversion are 2167, 2080, 1940, and 1767 Hz for the PM1, PM2, W5, and 3-9-19 sequences, respectively, corresponding to an increase in the inversion bandwidth of 400 Hz for PM1 and 313 Hz for PM2, compared with the 3-9-19 sequence. The frequency width of the suppression region which produces less than 10% of the intensity are 440, 410, 376 and 566 Hz for the PM1, PM2, W5, and 3-9-19 sequences, respectively, which are equivalent to narrowing the suppression region by 22% for PM1 and 28% for PM2, compared with the 3-9-19 sequence. For the experimental profiles with $\gamma B_1/2\pi = 32$ kHz for binomial-like sequences (Fig. 4), the resulting frequency widths which provide better than 90% inversion are 2233, 2410, 2500 and 1890 Hz for the PM1, PM2, W5, and 3-9-19 sequences, respectively, corresponding to an increase in the inversion bandwidth of 343 Hz for PM1 and 520 Hz for PM2, compared with the 3-9-19 sequence; while the frequency width of the suppression region which produces less than 10% of the intensity is essentially unaffected by increasing the RF power. Compared with the simulated profiles, the experimental profiles have slight intensity distortions at low RF power (Fig. 3) and these are due to resonance offset effects during the application of RF pulses which were assumed to be negligible in the design of the binomial-like sequences. These distortions were minimized by using high RF power for the binomial-like sequences (Fig. 4), except for the PM1 sequence, which was found to be more susceptible to resonance offset effects due to the use of longer RF pulses. The experimental profiles give wider suppression regions due to the use of excitation-sculpting [4]. The two new sequences provide selectivity similar to that of the W5 sequence but with far shorter durations. For example, when $\gamma B_1/2\pi = 12$ kHz and $\tau = 300$ μ s, the durations of the PM1, PM2, and 3-9-19 inverse pulses are 1.824, 1.617, and 1.6 ms, respectively, while the duration of the W5 inverse pulse is 2.825 ms. Therefore, the PM1 and PM2 sequences result in less signal attenuation by spin-spin relaxation than the W5 sequence.

As mentioned in Section 2, only the “z” magnetization has been taken into account during all the simulations, and therefore the newly obtained sequences may introduce phase distortions. To show the phase gradient (i.e., frequency dependent phase shift), a simulation was conducted, in which the PM1 binomial-like sequence was applied to a transverse magnetization vector shifted 45° away from the positive *x* axis. As shown in Fig. 5A, the PM1 binomial-like sequence causes a significant frequency dependent phase shift. To demonstrate the phase distortions, the PM1-based WATERGATE sequence has been applied to the lysozyme sample (Fig. 5B). The PM2 sequence also causes phase distortions (results not shown).

However, as mentioned in Section 1, the excitation sculpting and PGSTE-WATERGATE sequences can remove phase distortions caused by the use of soft pulses [8,9]. Therefore, in combination with excitation sculpting and PGSTE-WATERGATE, the utility of the new binomial-like sequences is demonstrated on the lysozyme

sample. As shown in Fig. 6, pure-phase spectra have been obtained for both of the new sequences. The greater inversion width and selectivity of the two new binomial-like sequences compared with the 3-9-19 sequence is evident by comparing the intensity of the peaks in the regions a, b, and c. In combination with PGSTE-WATERGATE, the new binomial-like sequences have been used in diffusion experiments on the lysozyme sample. As shown in Fig. 7, both of the new binomial-like sequences show great selectivity in PGSTE-WATERGATE experiments.

5. Conclusions

In combination with excitation sculpting, both of the new sequences outperform the 3-9-19 sequence in selectivity and inversion width. With significantly shorter durations, the new sequences provide similar selectivity and inversion width to the W5 sequence. When used in PGSTE-WATERGATE, they afford highly selective solvent suppression in diffusion experiments.

Acknowledgments

This research was supported by an Endeavour International Postgraduate Research Scholarship from the University of Western Sydney and the Australian government (G.Z.), and a NSW BioFirst Award from NSW Ministry for Science & Medical Research (W.S.P.).

References

- [1] P.J. Hore, A new method for water suppression in the proton NMR spectra of aqueous solutions, *J. Magn. Reson.* 54 (1983) 539–542.
- [2] P.J. Hore, Solvent suppression in Fourier transform nuclear magnetic resonance, *J. Magn. Reson.* 55 (1983) 283–300.
- [3] V. Sklenář, M. Piotto, R. Leppik, V. Saudek, Gradient-tailored water suppression for ¹H–¹⁵N HSQC experiments optimized to retain full sensitivity, *J. Magn. Reson., Ser. A* 102 (1993) 241–245.
- [4] M.L. Liu, X.A. Mao, C.H. Ye, H. Huang, J.K. Nicholson, J.C. Lindon, Improved WATERGATE pulse sequences for solvent suppression in NMR spectroscopy, *J. Magn. Reson.* 132 (1998) 125–129.
- [5] M. Piotto, V. Saudek, V. Sklenář, Gradient-tailored excitation for single-quantum NMR spectroscopy of aqueous solutions, *J. Biomol. NMR* 2 (1992) 661–665.
- [6] A.L. Davis, S. Wimperis, A solvent suppression technique giving NMR spectra with minimal amplitude and phase distortion, *J. Magn. Reson.* 84 (1989) 620–626.
- [7] D. Thomasson, D. Purdy, J.P. Finn, Phase-modulated binomial RF pulses for fast spectrally-selective musculoskeletal imaging, *Magn. Reson. Med.* 35 (1996) 563–568.
- [8] T.L. Hwang, A.J. Shaka, Water suppression that works. Excitation sculpting using arbitrary wave-forms and pulsed-field gradients, *J. Magn. Reson., Ser. A* 112 (1995) 275–279.
- [9] G. Zheng, T. Stait-Gardner, P.G. Anil Kumar, A.M. Torres, W.S. Price, PGSTE-WATERGATE: An STE-based PGSE NMR sequence with excellent solvent suppression, *J. Magn. Reson.* 191 (2008) 159–163.
- [10] O.W. Sørensen, G.W. Eich, M.H. Levitt, G. Bodenhausen, R.R. Ernst, Product operator formalism for the description of NMR pulse experiments, *Prog. Nucl. Magn. Reson. Spectrosc.* 16 (1984) 163–192.
- [11] W.S. Price, F. Elwinger, C. Vigouroux, P. Stilbs, PGSE-WATERGATE, a new tool for NMR diffusion-based studies of ligand-macromolecule binding, *Magn. Reson. Chem.* 40 (2002) 391–395.
- [12] R. Freeman, Shaped radiofrequency pulses in high resolution NMR, *Prog. Nucl. Magn. Reson. Spectrosc.* 32 (1998) 59–106.
- [13] M.P. Hall, P.J. Hore, Computer-optimized solvent suppression, *J. Magn. Reson.* 70 (1986) 350–354.
- [14] G.A. Morris, A.C.T. Silveston, J.C. Waterton, Computer optimization of solvent suppression pulse sequences, *J. Magn. Reson.* 82 (1989) 97–108.